

See discussions, stats, and author profiles for this publication at: <https://www.researchgate.net/publication/231729274>

Synthesis and Structures of New Mixed–Metal Lanthanide/Magnesium Allyl Complexes

ARTICLE *in* ORGANOMETALLICS · SEPTEMBER 2005

Impact Factor: 4.13 · DOI: 10.1021/om0505155

CITATIONS

33

READS

17

4 AUTHORS, INCLUDING:



Luis Fernando Sánchez-Barba Merlo

King Juan Carlos University

54 PUBLICATIONS 1,391 CITATIONS

SEE PROFILE



Manfred Bochmann

University of East Anglia

302 PUBLICATIONS 8,888 CITATIONS

SEE PROFILE

Synthesis and Structures of New Mixed-Metal Lanthanide/Magnesium Allyl Complexes

Luis F. Sánchez-Barba,[†] David L. Hughes,[†] Simon M. Humphrey,[‡] and Manfred Bochmann^{*,†}

Wolfson Materials and Catalysis Center, School of Chemical Sciences and Pharmacy, University of East Anglia, Norwich, NR4 7TJ, U.K., and University Chemical Laboratory, University of Cambridge, Lensfield Road, Cambridge, CB2 1EW, U.K.

Received June 22, 2005

The reaction of $\text{LnI}_3(\text{THF})_n$ ($\text{Ln} = \text{La}$, $n = 4$; $\text{Ln} = \text{Y}$, $n = 3.5$) with 3 equiv of allylMgI in THF/1,4-dioxane proceeds in moderate yields to give the unexpected mixed-metal complexes $[\text{Ln}(\eta^3\text{-C}_3\text{H}_5)_3(\mu\text{-C}_4\text{H}_8\text{O}_2)\cdot\text{Mg}(\eta^1\text{-C}_3\text{H}_5)_2(\mu\text{-C}_4\text{H}_8\text{O}_2)_{1.5}]_\infty$ ($\text{Ln} = \text{La}$ **1**, Y **2**). By contrast, samarium iodide gives a salt containing a new allyl-bridged anion, $[\text{Mg}(\text{THF})_6][\text{Sm}_2(\eta^3\text{-C}_3\text{H}_5)_6(\mu\text{-}\eta^3\text{-C}_3\text{H}_5)_2\cdot\text{toluene}]$ (**3**), while neodymium iodide affords $[\text{Mg}(\text{THF})_6][\text{Nd}(\eta^3\text{-C}_3\text{H}_5)_4]_2\cdot 2\text{THF}$ (**4**) under the same reaction conditions. On reaction with a mild proton acid such as the diketimine 2-(2,6-diisopropylphenyl)amino-4-(2,6-diisopropylphenyl)imino-2-pentene, **3** is converted into $[\text{Mg}(\text{THF})_6][\text{Sm}(\eta^3\text{-C}_3\text{H}_5)_4]_2\cdot 2\text{THF}$ (**5**), alongside $\text{Sm}(\eta^3\text{-C}_3\text{H}_5)_2\{\kappa^3\text{-HC}(\text{MeCNC}_6\text{H}_3\text{iPr}_2\text{-2,6})_2\}$. The solid-state structures of **1** and **2** contain distorted trigonal-bipyramidal lanthanide centers with three η^3 -allyl ligands and distorted trigonal-bipyramidal magnesium centers with two η^1 -bonded allyls. Both metal centers are connected by bridging 1,4-dioxane molecules building a planar polymeric network. By contrast, **3** and **5** consist of well-defined discrete ions. Complex **3** contains an unprecedented type of binuclear anion containing two samarium centers bridged by an $\eta^3\text{:}\eta^3$ -allyl ligand, while the anion in **5** has distorted tetrahedral geometry.

Introduction

Since the discovery of the tris(cyclopentadienyl) derivatives of the lanthanide elements by Wilkinson and Birmingham in the 1950s,¹ most of the organolanthanide compounds prepared during the last two decades have been sandwich complexes, a consequence of their relatively high stability. By contrast, cyclopentadienyl-free organolanthanide compounds are much less common. Several examples of homoleptic allyl-lanthanide complexes have been shown to be excellent precatalysts for polymerization reactions.² For instance, Taube et al.^{2a} reported the synthesis of the first neutral tris(η^3 -allyl)lanthanide complexes $[\text{La}(\eta^3\text{-C}_3\text{H}_5)_3(\kappa^1\text{-dioxane})]_2(\mu\text{-dioxane})$ and $[\text{Nd}(\eta^3\text{-C}_3\text{H}_5)_3(\mu\text{-dioxane})]_\infty$, which catalyze the 1,4-*trans*-polymerization of butadiene in toluene with high 1,4-*trans*-stereoselectivity. High syndiospecific polymerization of styrene has recently been

shown by allyl-lanthanide complexes.³ Lanthanide allyls stabilized by silyl substituents have been used in the polymerization of butadiene and of polar monomers; for example, we showed recently that silyl-substituted *ansa*-bis(allyl) lanthanide complexes and allyl-bridged oligonuclear complexes are highly active single-component catalysts for the polymerization of methyl methacrylate, butadiene, and cyclic esters.^{4,5} We have also reported⁶ that the reaction between $\text{LnCl}_3(\text{THF})_3$ ($\text{Ln} = \text{Y}$, Sm) and 3 equiv of allylmagnesium chloride affords the new homoleptic tris(allyl) complexes $[\text{Ln}(\eta^3\text{-C}_3\text{H}_5)_3(\mu\text{-dioxane})]_\infty$ ($\text{Ln} = \text{Y}$, Sm) in very good yields, in simple one-pot reactions. Recent advances have been summarized in excellent reviews including synthesis, structural chemistry, and ligand design in “non-cyclopentadienyl” organolanthanides.⁷

Tris(η^3 -allyl)lanthanides are promising starting materials. In an effort to develop an improved synthetic route, we investigated the reactions of analogous metal iodides and reacted $\text{LnI}_3(\text{THF})_n$ ($\text{Ln} = \text{La}$, $n = 4$; $\text{Ln} = \text{Y}$, Sm , Nd , $n = 3.5$) with allylmagnesium iodide. Quite unexpectedly, the products were rather different from

* Corresponding author. E-mail: M.Bochmann@uea.ac.uk.

[†] University of East Anglia.

[‡] University of Cambridge.

(1) Wilkinson, G.; Birmingham, J. M. *J. Am. Chem. Soc.* **1954**, *76*, 6210.

(2) (a) Taube, R.; Windisch, H.; Maiwald, S.; Hemling, H.; Schumann, H. *J. Organomet. Chem.* **1996**, *513*, 49. (b) Taube, R.; Windisch, H.; Weissenborn, H.; Hemling, H.; Schumann, H. *J. Organomet. Chem.* **1997**, *548*, 229. (c) Maiwald, S.; Taube, R.; Hemling, H.; Schumann, H. *J. Organomet. Chem.* **1998**, *552*, 195. (d) Taube, R.; Windisch, H.; Hemling, H.; Schumann, H. *J. Organomet. Chem.* **1998**, *555*, 201. (e) Amberger, H.-D.; Reddmann, H.; Unrecht, B.; Edelmann, F. T.; Edelstein, N. M. *J. Organomet. Chem.* **1998**, *566*, 125. (f) Landmesser, H.; Berndt, H.; Kunath, D.; Lücke, B. *J. Mol. Catal.* **2000**, *162*, 257. (g) Taube, R.; Maiwald, S.; Sieler, J. *J. Organomet. Chem.* **2001**, *621*, 327.

(3) Kirillov, E.; Lehmann, C. W.; Razavi, A.; Carpentier, J.-F. *J. Am. Chem. Soc.* **2004**, *126*, 12240.

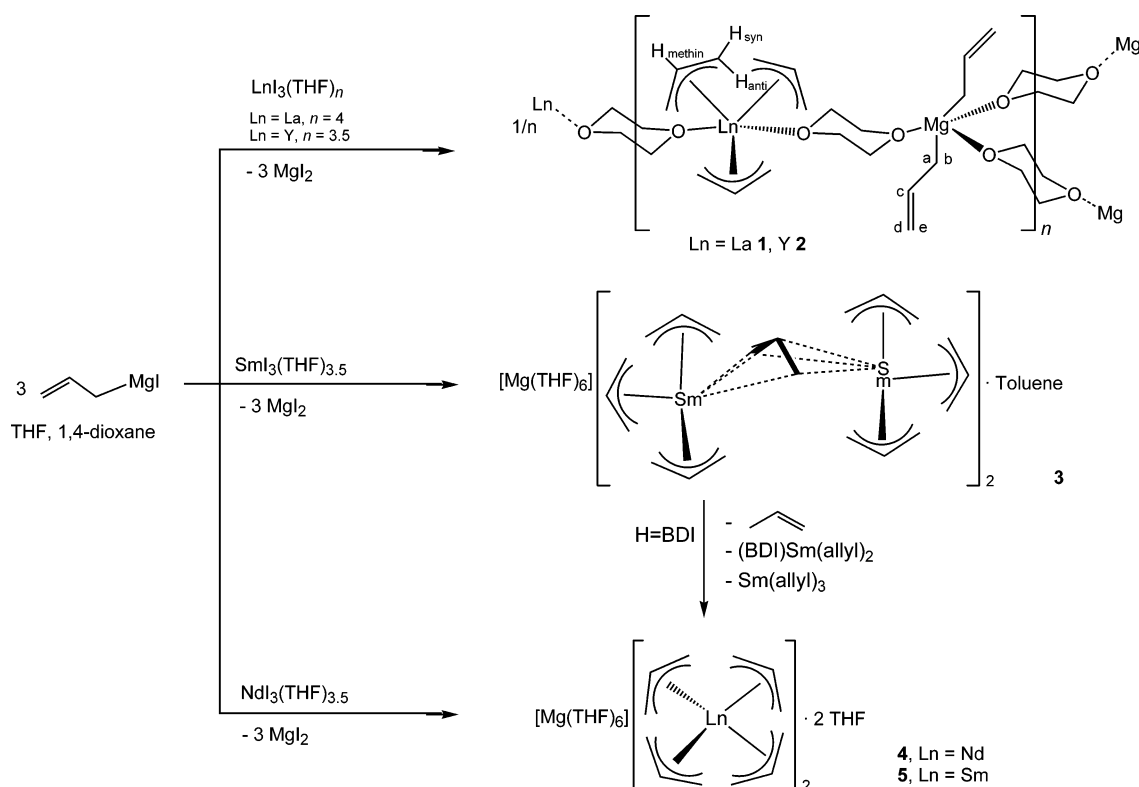
(4) (a) Woodman, T. J.; Schormann, M.; Hughes, D. L.; Bochmann, M. *Organometallics* **2003**, *22*, 3028. (b) Woodman, T. J.; Schormann, M.; Bochmann, M. *Organometallics* **2003**, *22*, 2938. (c) Woodman, T. J.; Schormann, M.; Hughes, D. L.; Bochmann, M. *Organometallics* **2004**, *23*, 2972.

(5) Woodman, T. J.; Schormann, M.; Hughes, D. L.; Bochmann, M. *Isr. J. Chem.* **2002**, *42*, 283.

(6) Sánchez-Barba, L. F.; Hughes, D. L.; Humphrey, S. M.; Bochmann, M. *Organometallics*, in press.

(7) (a) Edelmann, T. F.; Freckmann, M. M.; Schumann, H. *Chem. Rev.* **2002**, *102*, 1851. (b) Piers, W. E.; Emslie, D. J. *Coord. Chem. Rev.* **2002**, *233–234*, 129.

Scheme 1



those of the chloride route: depending on the metal, use of iodides leads either to group 3/magnesium mixed-metal allyl complexes (Ln = La or Y) or to new allyllanthanate anions (Ln = Sm, Nd). Similar attempts to prepare halide-free homoleptic allyl-lanthanide complexes from the bulky 1,3-bis(trimethylsilyl)allyl anion with lanthanide(III) iodides have failed, resulting instead in the formation of iodo complexes such as {1,3-C₃H₃(SiMe₃)₂}NdI₂(THF)_{1.25}⁵ and {1,3-C₃H₃(SiMe₃)₂}₂-NdI(THF)_n^{4c} or salts of the general formula [K(THF)₄][Ln{1,3-C₃H₃(SiMe₃)₂}₃] (Ln = Ce, Er, and Tb),⁸ despite the additional thermal stability that the application of this ligand imparts, demonstrated in previous studies.⁹

Results and Discussion

Synthesis. The reaction of LnI₃(THF)_n (Ln = La, *n* = 4; Ln = Y, Sm, Nd, *n* = 3.5) in a mixture of THF/1,4-dioxane (4:1) with 3 equiv of allylMgI at room temperature gave the unexpected η³/η¹-allyl mixed-metal neutral complexes [Ln(η³-C₃H₅)₃(μ-C₄H₈O₂)·Mg(η¹-C₃H₅)₂(μ-C₄H₈O₂)_{1.5}]_∞ (Ln = La 1, Y 2) in moderate yields as yellow and orange crystals, respectively. These compounds are neutral coordination polymers (Scheme 1).

By contrast, neodymium and samarium iodides behaved very differently under the same reaction conditions and afforded salts with discrete [Mg(THF)₆]²⁺ and allyl metalate ions, the red [Mg(THF)₆][Sm₂(η³-C₃H₅)₆(μ-η³:η³-C₃H₅)₂·toluene] (3) and the green [Mg(THF)₆][Nd(η³-C₃H₅)₄·2THF] (4). On reaction with a mild proton acid such as the diketimine ArN=C(Me)CH=

C(Me)NHAr (BDI-H, Ar = 2,6-C₆H₃iPr₂) in THF at 60 °C for 15 h, 3 was converted to [Mg(THF)₆][Sm(η³-C₃H₅)₄·2THF] (5), accompanied by the formation of the previously reported allyl complex Sm(η³-C₃H₅)₂{HC-(MeCNAr)₂}⁶ as well as Sm(η³-C₃H₅)₃.

The formation of these mixed-metal and ionic products from lanthanide *iodides* contrasts with the reactions of the corresponding lanthanide *trichlorides* LnCl₃(THF)_n (Ln = La, *n* = 4; Ln = Y, Sm, Nd, *n* = 3), which react with allylMgCl to give halide-free homoleptic tris(η³-allyl) complexes [La(η³-C₃H₅)₃(η¹-C₄H₈O₂)₂(μ-C₄H₈O₂)] and [Ln(η³-C₃H₅)₃(μ-C₄H₈O₂)]_∞ (Ln = Y, Sm, Nd).⁶ Evidently, slight changes in the starting materials and reaction conditions are responsible for this remarkable change in product composition. This is further exemplified by Taube's report a few years ago that the reaction of NdI₃(THF)_{3.5} and allylMgI afforded [Nd(η³-C₃H₅)₃(μ-C₄H₈O₂)]_∞.^{2g} In that preparation 1,4-dioxane was absent in the first stage of the reaction and consequently led to a different reaction pathway from the one observed here.

The new compounds 1–5 were characterized by NMR spectroscopy (¹H and ¹³C{¹H} for diamagnetic species) and elemental analyses. In complexes 1 and 2, the ¹H and ¹³C{¹H} NMR spectra in THF-*d*₈ at room temperature displayed one set of signals for the η³-allyl groups, showing the equivalence of H_{syn} and H_{anti} and a single sharp singlet for the bridging 1,4-dioxane molecules. The allyl groups coordinated to magnesium gave a pattern consistent with η¹-coordination, i.e., diastereotopic methylene protons H_a and H_b, the methine proton H_c, and two =CH₂ signals H_d and H_e. This pattern is in agreement with a polymeric structure with η³- and η¹-bonded allyl groups and bridging 1,4-dioxane molecules (Scheme 1). These compounds are extremely

(8) Kuehl, C. J.; Simpson, C. K.; John, K. D.; Sattelberger, A. P.; Carlson, C. N.; Hanusa, T. P. *J. Organomet. Chem.* **2003**, 683, 149.

(9) (a) Harvey, M. J.; Hanusa, T. P.; Young, V. G. Jr. *Angew. Chem., Int. Ed.* **1999**, 38, 217. (b) Smith, J. D.; Hanusa, T. P.; Young, V. G., Jr. *J. Am. Chem. Soc.* **2001**, 123, 6455.

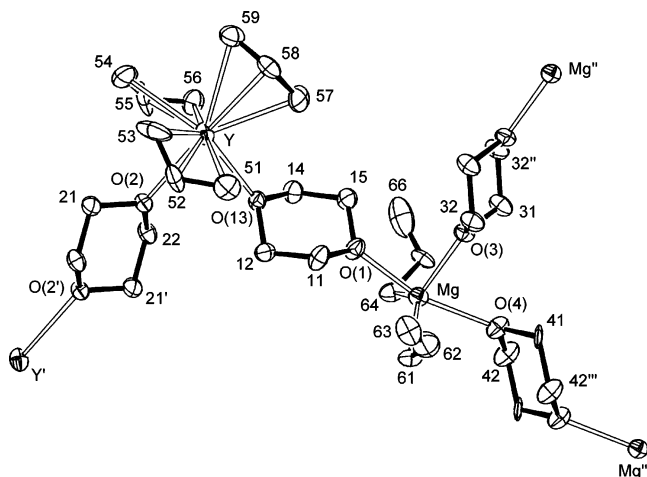


Figure 1. View of a fragment of the planar polymer network in complex $[Y(\eta^3\text{-C}_3\text{H}_5)_3(\mu\text{-C}_4\text{H}_8\text{O}_2)\text{Mg}(\eta^1\text{-C}_3\text{H}_5)_2(\mu\text{-C}_4\text{H}_8\text{O}_2)_{1.5}]_\infty$ (**2**). Hydrogen atoms have been omitted for clarity. Thermal ellipsoids are drawn at the 50% probability level. The lanthanum analogue **1** is isostructural.

air- and moisture-sensitive. They are highly soluble in THF or 1,4-dioxane, are insoluble in light petroleum, toluene, or diethyl ether, and decompose in dichloromethane.

Structural Studies. Whereas single crystals of **1**, **2**, and **4** suitable for X-ray diffraction crystallography were readily grown from 1,4-dioxane/toluene at -26°C , the isolation of crystals for the samarium derivative **3** was complicated by the extreme sensitivity and relative instability of this compound. The smallest crystals decomposed almost immediately when removed from the Schlenk tube under nitrogen, whereas the bigger ones degraded on the diffractometer during the course of data acquisition. Suitable crystals of **3** were eventually obtained by recrystallization from a 1:8 mixture of 1,4-dioxane/toluene after several days at -26°C .

Complexes **1** and **2** are isostructural and present essentially the same arrangement, as shown in Figure 1 for compound **2**. The bond lengths and angles are very similar in the two molecules (Table 1).

The structures confirm the presence of three η^3 -allyl groups. If one considers the allyl ligands as occupying one coordination site, the geometry of the lanthanide metal center is a distorted trigonal bipyramid, in which O(2) and the allyl group of C(58) are the axial groups. The magnesium centers also form distorted trigonal bipyramids but contain two η^1 -allyl ligands in the equatorial plane, with the 1,4-dioxane ligands of O(1) and O(4) in axial positions. Finally, bridging chair-shaped 1,4-dioxane rings linking the $\text{Ln}(\eta^3\text{-C}_3\text{H}_5)_3$ and $\text{Mg}(\eta^1\text{-C}_3\text{H}_5)_2$ units build a planar polymeric network. The 1,4-dioxane group that links the Ln and Mg atoms, i.e., that of O(13), does not show precise symmetry; all the other dioxane molecules, which form links between pairs of Ln atoms, i.e. those of O(2), and between pairs of Mg atoms, i.e. those of O(3) and O(4), lie on centers of symmetry.

The O(2)–Ln–C(58) moieties are almost linear, with O(2)–La(1)–C(58) = $171.47(18)^\circ$ and O(2)–Y–C(58) = $174.4(4)^\circ$. The η^3 -allyl ligands in **2** display Y–C distances in the range 2.525(11)–2.770(9) Å. The La–C distances in the **1** are significantly longer, at 2.731(6)–2.827(6) Å, reflecting the differences in ionic radii. Some

Table 1. Selected Interatomic Distances (Å) and Angles (deg) in Compounds **1** and **2** (esd's are in parentheses)

	compound 1 , Ln = La	compound 2 , Ln = Y
Ln(1)–O(13)	2.653(4)	2.513(3)
Ln(1)–O(2)	2.662(3)	2.549(3)
Ln(1)–C(51)	2.794(6)	2.600(8)
Ln(1)–C(52)	2.827(6)	2.589(8)
Ln(1)–C(53)	2.756(6)	2.525(11)
Ln(1)–C(54)	2.815(7)	2.770(9)
Ln(1)–C(55)	2.806(8)	2.704(9)
Ln(1)–C(56)	2.739(6)	2.686(8)
Ln(1)–C(57)	2.731(6)	2.622(5)
Ln(1)–C(58)	2.783(6)	2.645(5)
Ln(1)–C(59)	2.763(6)	2.709(5)
Mg(1)–O(1)	2.191(4)	2.201(4)
Mg(1)–O(3)	2.161(4)	2.158(3)
Mg(1)–O(4)	2.338(4)	2.350(5)
Mg(1)–C(61)	2.197(6)	2.189(8)
Mg(1)–C(64)	2.195(6)	2.188(8)
O(13)–Ln(1)–O(2)	73.34(11)	72.31(10)
O(13)–Ln(1)–C(52)	101.59(17)	104.0(2)
O(13)–Ln(1)–C(55)	102.5(3)	102.3(4)
O(13)–Ln(1)–C(58)	106.08(17)	107.60(15)
O(2)–Ln(1)–C(52)	73.30(15)	76.4(4)
O(2)–Ln(1)–C(55)	70.7(3)	68.7(4)
O(2)–Ln(1)–C(58)	171.47(18)	174.4(4)
O(3)–Mg(1)–O(1)	82.14(15)	82.85(14)
O(1)–Mg(1)–O(4)	165.25(16)	165.3(3)
O(1)–Mg(1)–C(61)	96.5(2)	96.6(6)
O(1)–Mg(1)–C(64)	92.9(2)	92.6(6)
O(3)–Mg(1)–O(4)	83.73(15)	83.21(14)
O(3)–Mg(1)–C(61)	112.0(2)	114.0(8)
O(3)–Mg(1)–C(64)	117.5(2)	115.7(8)
C(61)–Mg(1)–O(4)	92.7(2)	93.3(4)
C(64)–Mg(1)–O(4)	89.9(2)	89.2(5)
C(61)–Mg(1)–C(64)	130.3(2)	130.2(2)
C(51)–C(52)	1.387(9)	1.380(11)
C(52)–C(53)	1.384(9)	1.348(14)
C(61)–C(62)	1.452(8)	1.458(9)
C(62)–C(63)	1.322(9)	1.320(9)
C(53)–C(52)–C(51)	126.4(6)	123.5(9)
C(62)–C(61)–Mg(1)	117.0(4)	114.8(14)
C(63)–C(62)–C(61)	130.0(7)	143.7(18)
C(65)–C(64)–Mg(1)	116.5(4)	113.6(12)
C(66)–C(65)–C(64)	128.0(7)	118.0(16)

of the bond angles of central allyl C atoms deviate significantly from sp^2 hybridization, viz., the angle C(54)–C(55)–C(56) = $137.0(10)^\circ$ and $136.2(12)^\circ$, for lanthanum and yttrium, respectively. The magnesium metal center presents the two allyl groups η^1 -bonded with similar Mg–C bond lengths in both complexes. The O(1)–Mg–O(4) angle approaches linearity, $165.25(16)^\circ$ in **1** and $165.3(3)^\circ$ in **2**. The Mg(1)–O(4) bond lengths are significantly longer than Mg(1)–O(3) and Mg(1)–O(1) in both complexes. Finally, in the η^1 -allyl ligands, too, the angles around the central carbon atom C(62) deviate from 120° , i.e., C(61)–C(62)–C(63) = $130.0(7)^\circ$ and $143.7(18)^\circ$, for **1** and **2**, respectively.

The packing diagram of **1** and **2** (Figure 2) shows sheets of parallel zigzag chains Mg–dioxane–Mg–dioxane–Mg–... across centers of symmetry, linked by –dioxane–Ln($\eta^3\text{-C}_3\text{H}_5$)₃–dioxane–Ln($\eta^3\text{-C}_3\text{H}_5$)₃–dioxane– units, to give dioxane-linked Mg_6Ln_4 macrocycles. The network has the appearance of a square grid with some links absent; there is a metal atom at every junction, with a right-angle turn in the chain at every Ln atom and a T-junction at every Mg atom.

The single-crystal X-ray structure of **3** (Figure 3) confirms the presence of discrete ions. Selected dimensions are listed in Table 2. The binuclear anion involves

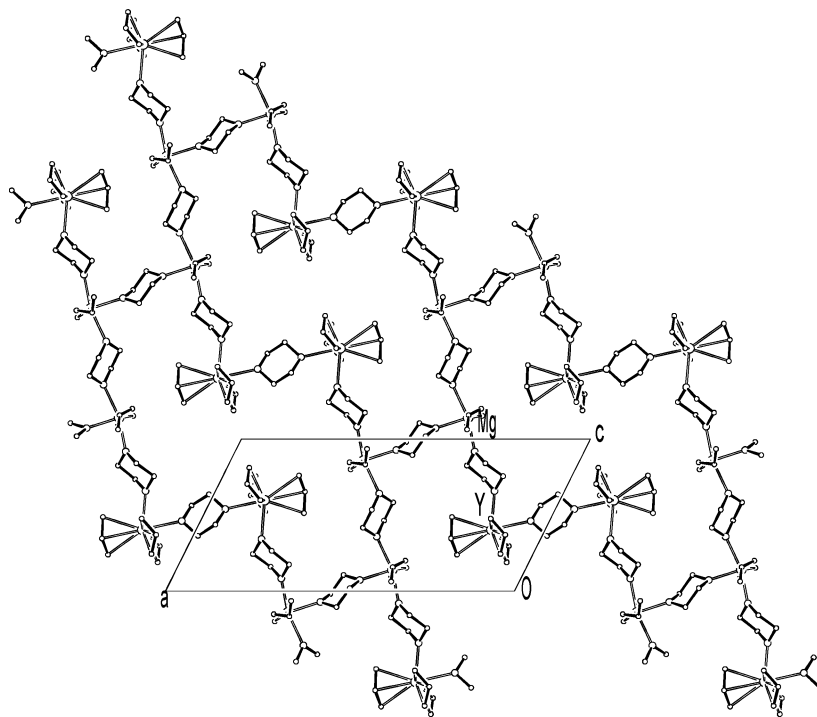


Figure 2. Projection of the planar polymeric chains down the *b*-axis in complex **2**; complex **1** is essentially identical.

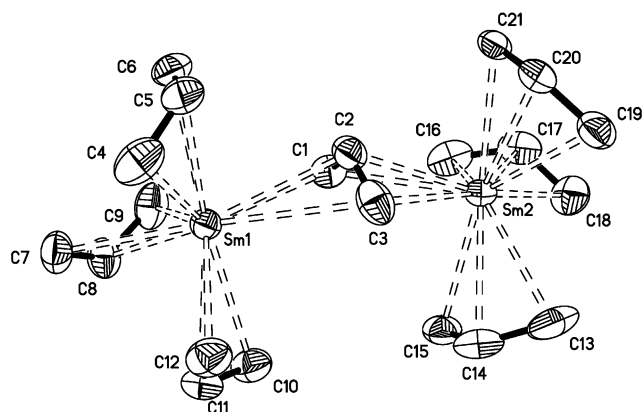


Figure 3. X-ray structure of the anion $[\text{Sm}_2(\eta^3\text{-C}_3\text{H}_5)_6(\mu\text{-}\eta^3\text{:}\eta^3\text{-C}_3\text{H}_5)]^-$ (**3**[−]) showing the atomic numbering scheme. Hydrogen atoms have been omitted for clarity. Thermal ellipsoids are drawn at the 50% probability level.

two samarium centers in distorted tetrahedral arrangements, with three terminal and one bridging η^3 -allyl ligand. To our knowledge, **3** constitutes the first authenticated example of this type of structure.¹⁰

Both samarium centers are bonded to three η^3 -allyl ligands, all with rather similar Sm–C bond lengths of 2.623(5)–2.725(5) Å. The bridging allyl group is symmetrically $\eta^3\text{:}\eta^3$ -bonded and shows significantly longer Sm–C distances of 2.762(6)–2.977(6) Å. The C–C bond lengths differ little between the allyl ligands, with an average of 1.375(2) Å. All the central carbon atoms show C–C angles expected for sp^2 hybridization, 126.1(6)–127.0(6)°, with a slightly wider angle for the bridging allyl [$\text{C}(1)\text{--C}(2)\text{--C}(3) = 129.0(6)^\circ$].

By contrast, the crystal structure of **4** showed that this compound contained the $[\text{Nd}(\eta^3\text{-allyl})_4]^-$ anion.

Table 2. Selected Interatomic Distances (Å) and Angles (deg) for **3**

Sm(1)–C(1)	2.793(6)	Sm(2)–C(1)	2.774(6)
Sm(1)–C(2)	2.762(6)	Sm(2)–C(2)	2.765(6)
Sm(1)–C(3)	2.977(6)	Sm(2)–C(3)	2.972(6)
Sm(1)–C(4)	2.675(5)	Sm(2)–C(13)	2.699(5)
Sm(1)–C(5)	2.700(5)	Sm(2)–C(14)	2.712(5)
Sm(1)–C(6)	2.680(5)	Sm(2)–C(15)	2.712(5)
Sm(1)–C(7)	2.725(5)	Sm(2)–C(16)	2.655(5)
Sm(1)–C(8)	2.710(5)	Sm(2)–C(17)	2.717(5)
Sm(1)–C(9)	2.651(5)	Sm(2)–C(18)	2.712(6)
Sm(1)–C(10)	2.713(5)	Sm(2)–C(19)	2.632(5)
Sm(1)–C(11)	2.701(5)	Sm(2)–C(20)	2.691(5)
Sm(1)–C(12)	2.623(5)	Sm(2)–C(21)	2.673(5)
C(5)–Sm(1)–C(2)	78.97(18)	C(14)–Sm(2)–C(2)	97.66(19)
C(8)–Sm(1)–C(2)	133.37(17)	C(17)–Sm(2)–C(2)	128.57(18)
C(11)–Sm(1)–C(2)	117.55(18)	C(20)–Sm(2)–C(2)	78.60(17)
C(5)–Sm(1)–C(8)	121.71(18)	C(14)–Sm(2)–C(17)	119.31(18)
C(5)–Sm(1)–C(11)	133.23(18)	C(20)–Sm(2)–C(14)	128.03(16)
C(11)–Sm(1)–C(8)	80.18(18)	C(20)–Sm(2)–C(17)	100.93(17)
C(1)–C(2)	1.369(7)	C(11)–C(12)	1.381(7)
C(2)–C(3)	1.370(8)	C(13)–C(14)	1.385(9)
C(4)–C(5)	1.370(8)	C(14)–C(15)	1.363(8)
C(5)–C(6)	1.379(8)	C(16)–C(17)	1.371(9)
C(7)–C(8)	1.382(8)	C(17)–C(18)	1.379(8)
C(8)–C(9)	1.380(8)	C(19)–C(20)	1.370(7)
C(10)–C(11)	1.372(8)	C(20)–C(21)	1.384(7)
C(1)–C(2)–C(3)	129.0(6)	C(15)–C(14)–C(13)	127.0(6)
C(4)–C(5)–C(6)	126.1(6)	C(16)–C(17)–C(18)	127.0(6)
C(9)–C(8)–C(7)	126.2(6)	C(19)–C(20)–C(21)	126.6(5)
C(10)–C(11)–C(12)	125.6(6)		
Mg(1)–O(1)	2.119(3)	O(1)–Mg(1)–O(2)	90.80(11)
Mg(1)–O(2)	2.127(3)	O(3)–Mg(1)–O(1)	89.49(12)
Mg(1)–O(3)	2.082(3)	O(3)–Mg(1)–O(2)	90.69(11)

Anions of this type have been previously established by Taube et al. in the case of $[\text{Li}(\mu\text{-dioxane})_{1.5}][\text{Ln}(\eta^3\text{-C}_3\text{H}_5)_4]$ (Ln = La, Nd)^{2a} and will therefore not be discussed here in detail.

As discussed above, protolysis of **3** resulted in the formation of **5**. The crystal structure confirmed the presence of the $[\text{Sm}(\eta^3\text{-allyl})_4]^-$ anion (Figure 4). Se-

(10) (a) Bailey, P. M.; Keasey, A.; Maitlis, P. M. *J. Chem. Soc., Dalton Trans.* **1978**, 1825. (b) Bobbie, B. J.; Taylor, N. J.; Carty, A. J. *Chem. Commun.* **1991**, 1511.

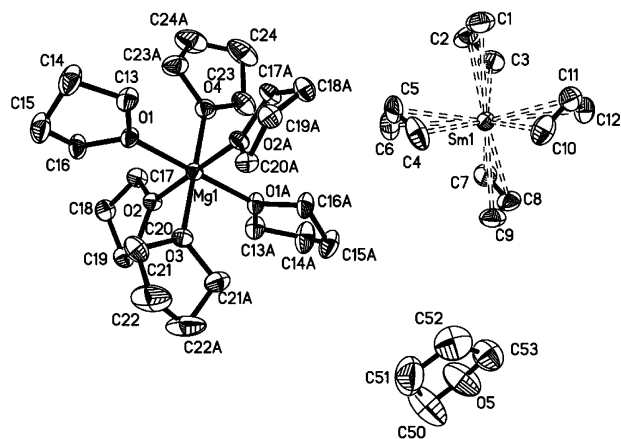


Figure 4. X-ray structure of the complex $[\text{Mg}(\text{THF})_6][\text{Sm}(\eta^3\text{-C}_3\text{H}_5)_4]_2 \cdot 2\text{THF}$ (**5**) showing the atomic numbering scheme. The cation lies about a 2-fold symmetry axis, and hence only half is present in the asymmetric unit of **5**. Hydrogen atoms have been omitted for clarity. Thermal ellipsoids are drawn at the 50% probability level.

Table 3. Selected Interatomic Distances (Å) and Angles (deg) in Complex **5**^a

(a) About the Samarium Atom			
Sm(1)–C(1)	2.761(5)	Sm(1)–C(7)	2.739(5)
Sm(1)–C(2)	2.708(4)	Sm(1)–C(8)	2.738(4)
Sm(1)–C(3)	2.648(4)	Sm(1)–C(9)	2.734(4)
Sm(1)–C(4)	2.673(4)	Sm(1)–C(10)	2.709(4)
Sm(1)–C(5)	2.712(5)	Sm(1)–C(11)	2.736(4)
Sm(1)–C(6)	2.751(5)	Sm(1)–C(12)	2.743(4)
C(2)–Sm(1)–C(5)	81.29(17)	C(2)–Sm(1)–C(8)	128.78(17)
C(2)–Sm(1)–C(11)	99.42(17)	C(5)–Sm(1)–C(8)	119.86(16)
C(5)–Sm(1)–C(11)	124.68(17)	C(11)–Sm(1)–C(8)	102.53(14)
(b) About the Magnesium Atom			
Mg(1)–O(1)	2.084(2)	Mg(1)–O(3)	2.110(4)
Mg(1)–O(2)	2.076(2)	Mg(1)–O(4)	2.130(4)
O(2')–Mg(1)–O(2)	178.98(15)	O(2)–Mg(1)–O(4)	90.51(8)
O(2)–Mg(1)–O(1)	90.77(10)	O(1)–Mg(1)–O(3)	90.34(8)
O(1')–Mg(1)–O(1)	179.32(17)	O(1)–Mg(1)–O(4)	89.66(8)
O(2)–Mg(1)–O(3)	89.49(8)	O(3)–Mg(1)–O(4)	180.0
(c) In the Allyl Ligands			
C(1)–C(2)	1.392(8)	C(7)–C(8)	1.369(6)
C(2)–C(3)	1.339(7)	C(8)–C(9)	1.383(6)
C(4)–C(5)	1.390(7)	C(10)–C(11)	1.385(6)
C(5)–C(6)	1.376(8)	C(11)–C(12)	1.377(6)
C(3)–C(2)–C(1)	129.9(6)	C(7)–C(8)–C(9)	126.4(5)
C(6)–C(5)–C(4)	126.5(5)	C(12)–C(11)–C(10)	126.6(5)

^a Symmetry transformation used to generate equivalent atoms: ' : 1–x, y, 1/2–z.

lected geometric parameters are listed in Table 3. The anion contains four η^3 -allyl ligands, three of which are rather asymmetrically bonded; for example, in the ligand C(1)–C(2)–C(3) the Sm–C distances range from 2.648(4) to 2.761(5) Å. By contrast, the Sm–C distances to C(7)–C(8)–C(9) are almost identical.

Conclusions

The reactions of group 3 and lanthanide metal halides with allylmagnesium halides in THF/dioxane mixtures were found to be surprisingly sensitive to both the nature of the metal and the halide, with chlorides producing the expected $\text{Ln}(\eta^3\text{-allyl})_3$ complexes, while the analogous iodides afforded magnesium-lanthanide mixed-metal products. While the lanthanum and yttrium allyls thus formed exist as neutral, dioxane-bridged coordination polymers in which a $\text{Mg}(\eta^1\text{-allyl})_2$ -

(dioxane)₂ zigzag chain is bridged by dioxane{ $\text{Ln}(\eta^3\text{-allyl})_3(\text{dioxane})_2$ } units, samarium and neodymium give ionic products containing $[\text{Nd}(\eta^3\text{-allyl})_4]^-$ and the new binuclear $[\text{Sm}_2(\eta^3\text{-allyl})_6(\mu\text{-}\eta^3\text{-}\eta^3\text{-allyl})]^-$ anion. Protolysis of the latter results in the formation of $[\text{Sm}(\eta^3\text{-allyl})_4]^-$. The reactivity of these readily accessible starting materials will be reported elsewhere.

Experimental Section

General Procedures. All manipulations were performed under nitrogen, using standard Schlenk techniques. Solvents were predried over sodium wire (toluene, light petroleum, THF, diethyl ether) or calcium hydride (dichloromethane) and distilled under nitrogen from sodium (toluene), sodium–potassium alloy (light petroleum, bp 40–60 °C), sodium–benzophenone (THF, diethyl ether), or calcium hydride (dichloromethane). Deuterated solvents were stored over activated 4 Å molecular sieves and degassed by several freeze–thaw cycles. Rare earth metal powder was purchased (Aldrich Chemical Co). Anhydrous LnCl_3 was prepared according to the literature procedures. Lanthanide iodides $\text{LnI}_3(\text{THF})_n$ were prepared by Soxhlet extraction of LnI_3 with THF for several days. NMR spectra were recorded using a Bruker Avance DPX-300 spectrometer. ¹H NMR spectra (300.1 MHz) were referenced to the residual solvent proton of the deuterated solvent used. ¹³C NMR spectra (75.5 MHz) were referenced internally to the D-coupled ¹³C resonances of the NMR solvent.

Preparation of $[\text{La}(\eta^3\text{-C}_3\text{H}_5)_3(\mu\text{-C}_4\text{H}_8\text{O}_2)\text{Mg}(\eta^1\text{-C}_3\text{H}_5)_2(\mu\text{-C}_4\text{H}_8\text{O}_2)]_{1.5}]_{\infty}$ (1**).** To a solution of $\text{LaI}_3(\text{THF})_4$ (1 g, 1.23 mmol) in THF (100 mL) was added dropwise a solution of allylMgI in THF (0.475 M, 7.82 mL, 3.71 mmol) at room temperature and 1,4-dioxane (25 mL). The initial pale brown solution became yellow over time. The resulting yellow suspension was stirred at room temperature for 12 h. After filtration and removal of volatiles, the yellow oily residue was extracted with 1,4-dioxane (10 mL) and filtrated. On addition of toluene (60 mL) and cooling to –26 °C, **1** was isolated as a yellow microcrystalline solid, yield 0.27 g (0.45 mmol, 61.7%). Anal. Calcd for $\text{C}_{25}\text{H}_{45}\text{O}_5\text{MgLa}$: C, 50.94; H, 7.64. Found: C, 51.03; H, 7.66. ¹H NMR (THF-*d*₈, 20 °C; for atom labels see Scheme 1): δ 6.00 (m, 3 H_{methine}, CH_2CHCH_2), 5.80 (m, 2 H_c, $-\text{CH}_2\text{CHCH}_2$), 5.01 (dm, $J_{\text{HH}} = 18.3$ Hz, 1 H_e, $\text{MgCH}_2\text{CHCH}_2$), 4.91 (dm, $J_{\text{HH}} = 12.1$ Hz, 1 H_d, $\text{MgCH}_2\text{CHCH}_2$), 3.54 (s, 8 H, $\mu\text{-C}_4\text{H}_8\text{O}_2$), 3.09 (d, $J_{\text{HH}} = 6.1$ Hz, 6 H_{syn}, CH_2CHCH_2), 2.25 (d, $J_{\text{HH}} = 15.1$ Hz, 6 H_{anti}, CH_2CHCH_2), 1.68 (m, 1 H_a, $\text{MgCH}_2\text{CHCH}_2$), 1.67 (m, 1 H_b, $\text{MgCH}_2\text{CHCH}_2$). ¹³C NMR (THF-*d*₈, 20 °C): δ 145.9 (CH_2CHCH_2), 134.2 ($-\text{CH}_2\text{CHCH}_2$), 116.0 ($-\text{CH}_2\text{CHCH}_2$), 70.1 (CH_2CHCH_2), 67.9 ($\mu\text{-C}_4\text{H}_8\text{O}_2$), 19.5 ($-\text{CH}_2\text{CHCH}_2$).

Preparation of $[\text{Y}(\eta^3\text{-C}_3\text{H}_5)_3(\mu\text{-C}_4\text{H}_8\text{O}_2)\text{Mg}(\eta^1\text{-C}_3\text{H}_5)_2(\mu\text{-C}_4\text{H}_8\text{O}_2)]_{1.5}]_{\infty}$ (2**).** Following the procedure described for **1**, to a solution of $\text{YI}_3(\text{THF})_{3.5}$ (1 g, 1.38 mmol) in THF (100 mL) was added dropwise a solution of allylMgI in THF (0.475 M, 8.75 mL, 4.15 mmol) at room temperature and 1,4-dioxane (25 mL). The initial pale yellow solution became orange over time. The resulting orange suspension was stirred at room temperature for 12 h. After filtration and removal of volatiles, the orange oil was extracted with 1,4-dioxane (10 mL) and filtrated. Finally, toluene was added (60 mL). Cooling to –26 °C gave **2** as an orange microcrystalline solid, yield 0.28 g (0.52 mmol, 62.5%). Anal. Calcd for $\text{C}_{25}\text{H}_{45}\text{O}_5\text{MgY}$: C, 55.67; H, 8.35. Found: C, 55.63; H, 8.39. ¹H NMR (THF-*d*₈, 20 °C; for atom labels see Scheme 1): δ 6.23 (m, 3 H_{methine}, CH_2CHCH_2), 5.80 (m, 2 H_c, $\text{MgCH}_2\text{CHCH}_2$), 5.01 (dm, $J_{\text{HH}} = 18.3$ Hz, 1 H_e, $\text{MgCH}_2\text{CHCH}_2$), 4.91 (dm, $J_{\text{HH}} = 12.1$ Hz, 1 H_d,

Table 4. Crystal Data and Summary of Data Collection and Refinement Details for 1–3 and 5

	1	2	3	5
formula	C ₂₅ H ₄₅ LaMgO ₅	C ₂₅ H ₄₅ MgO ₅ Y	C ₄₂ H ₇₀ Sm ₄ , C ₂₄ H ₄₈ MgO ₆ , C ₇ H ₈	2(C ₁₂ H ₂₀ Sm), C ₂₄ H ₄₈ MgO ₆ , 2(C ₄ H ₈ O)
cryst size, mm	0.16 × 0.12 × 0.07	0.28 × 0.23 × 0.10	0.12 × 0.12 × 0.07	0.23 × 0.12 × 0.05
fw	588.83	538.8	1725.45	1230.40
cryst syst	monoclinic	monoclinic	monoclinic	monoclinic
space group	<i>P</i> 2 ₁ / <i>n</i> (equiv to no. 14)	<i>P</i> 2 ₁ / <i>a</i> (equiv to no. 14)	<i>P</i> 2 ₁ / <i>c</i> (no. 14)	<i>C</i> 2/ <i>c</i> (no. 15)
<i>a</i> , Å	10.8248(2)	22.0174(7)	12.3977(2)	23.3797(4)
<i>b</i> , Å	12.6089(3)	12.4833(6)	21.6574(2)	21.6107(4)
<i>c</i> , Å	20.0674(5)	10.7855(3)	14.9078(2)	12.3467(3)
β, deg	92.6808(10)	116.344(2)	104.4172(5)	103.2519(8)
<i>V</i> , Å ³	2735.98(11)	2656.53(17)	3876.72(9)	6072.1(2)
<i>Z</i>	4	4	2	4
<i>D</i> _{calcd} , Mg/m ³	1.430	1.347	1.478	1.346
μ, mm ^{−1}	1.614	2.250	3.038	1.972
<i>F</i> (000)	1216	1144	1744	2560
no. of indep. reflns	4792 (<i>R</i> _{int} = 0.073)	3176 (<i>R</i> _{int} = 0.065)	8859 (<i>R</i> _{int} = 0.061)	6915 (<i>R</i> _{int} = 0.053)
no. obsd reflns (<i>I</i> > 2σ _{<i>i</i>})	3439	2765	6490	5125
no. of data/restraints/params	4792/0/289	3176/12/293	8859/0/382	6915/0/304
goodness of fit	1.045	1.092	1.024	1.022
final <i>R</i> indices (all data)	<i>R</i> ₁ = 0.080, <i>wR</i> ₂ = 0.101 ^a	<i>R</i> ₁ = 0.055, <i>wR</i> ₂ = 0.102 ^a	<i>R</i> ₁ = 0.070, <i>wR</i> ₂ = 0.093 ^a	<i>R</i> ₁ = 0.066, <i>wR</i> ₂ = 0.084 ^a
final <i>R</i> indices (obs data)	<i>R</i> ₁ = 0.049, <i>wR</i> ₂ = 0.090 ^a	<i>R</i> ₁ = 0.043, <i>wR</i> ₂ = 0.096 ^a	<i>R</i> ₁ = 0.040, <i>wR</i> ₂ = 0.084 ^a	<i>R</i> ₁ = 0.039, <i>wR</i> ₂ = 0.075 ^a
weighting params <i>A</i> , <i>B</i> ^a	0.0200, 12.53	0.0394, 4.25	0.0389, 4.93	0.0212, 20.71
largest diff peak and hole, e Å ^{−3}	0.94, −0.77	0.99, −0.50	1.56, −1.57	0.92, −0.62

^a Reflections were weighted: $w = [\sigma^2(F_o^2) + (AP)^2 + BP]^{-1}$ with $P = (F_o^2 + 2F_c^2)/3$.

MgCH₂CHCH₂), 3.54 (s, 8 H, μ -C₄H₈O₂), 2.33 (d, *J*_{HH} = 9.6 Hz, 12 H_{syn-anti}, CH₂CHCH₂), 1.68 (m, 1 H_a, MgCH₂CHCH₂), 1.67 (m, 1 H_b, MgCH₂CHCH₂). ¹³C NMR (THF-*d*₈, 20 °C): δ 149.5 (CH₂CHCH₂), 134.2 (MgCH₂CHCH₂), 116.0 (MgCH₂CHCH₂), 67.9 (μ -C₄H₈O₂), 56.9 (CH₂CHCH₂), 19.5 (MgCH₂CHCH₂).

Preparation of [Mg(THF)₆][Sm₂(η^3 -C₃H₅)₆(μ - η^3 -C₃H₅)₂·toluene (3). Following the procedure described for **1**, to a solution of SmI₃(THF)_{3.5} (1 g, 1.27 mmol) in THF (100 mL) was added dropwise a solution of allylMgI in THF (0.475 M, 8.06 mL, 3.83 mmol) at room temperature and 1,4-dioxane (25 mL). The initial yellow solution changed immediately to dark red. The resulting dark red suspension was stirred at room temperature for 12 h. Workup gave **3** as a red microcrystalline solid, yield 1.12 g (0.65 mmol, 59.2%). Anal. Calcd for C₇₃H₁₂₆O₆MgSm₄: C, 50.76; H, 7.30. Found: C, 50.83; H, 7.36.

Preparation of [Mg(THF)₆][Nd(η^3 -C₃H₅)₄]₂·2THF (4). Following the procedure described for **1**, to a solution of NdI₃·(THF)_{3.5} (1 g, 1.28 mmol) in THF (100 mL) was added dropwise a THF solution of allylMgI (0.475 M, 8.12 mL, 3.86 mmol) at room temperature, as well as 1,4-dioxane (25 mL). The initial pale blue solution became green over time. Workup gave **4** as a dark green microcrystalline solid, yield 0.72 g (0.59 mmol, 61.2%). Anal. Calcd for C₅₆H₁₀₄O₈MgNd₂: C, 55.17; H, 8.53. Found: C, 55.23; H, 8.61.

Preparation of [Mg(THF)₆][Sm(η^3 -C₃H₅)₄]₂·2THF (5). To a solution of [Mg(THF)₆][Sm₂(η^3 -C₃H₅)₆(μ - η^3 -C₃H₅)₂·toluene (**3**, 1 g, 0.58 mmol) in THF (100 mL) was added dropwise a solution of ArN=C(Me)CH=C(Me)NHAr (BDI-H, Ar = 2.6-C₆H₃Pr₂) (0.24 g, 0.58 mmol) in THF at room temperature. The initial dark red solution became red over time. The resulting red solution was stirred at 60 °C for 15 h. After removing of the volatiles, the red solid was washed with light petroleum ether (10 mL). Finally, THF was added (10 mL) and the mixture was cooled to −26 °C, affording **5** as a red microcrystalline solid, yield 0.41 g (0.33 mmol, 57.4%). Anal. Calcd for C₅₆H₁₀₄O₈MgSm₂: C, 54.61; H, 8.45. Found: C, 54.70; H, 8.49.

X-ray Crystallography. Crystals coated with dry Nujol or perfluoropolyether were mounted on a glass fiber and fixed in the cold nitrogen steam (*T* = 180(2) K). Intensity data were collected on a Nonius KappaCCD diffractometer equipped with

a Mo K α radiation (λ = 0.71073 Å) and graphite monochromator. Data were processed using the DENZO/SCALEPACK programs¹² and absorption corrections applied in SORTAV.¹³ The structures were determined by direct methods in the SHELXS program¹⁴ and refined by full-matrix least-squares methods, on *F*² values, in SHELXL.¹⁵ The non-hydrogen atoms were refined with anisotropic thermal parameters. Hydrogen atoms were included in idealized positions, and their *U*_{iso} values set to ride on the *U*_{eq} values of the parent carbon atoms. Scattering factors for neutral atoms were taken from the literature.¹⁶ Computer programs used in this analysis have been noted above and were run on a DEC-AlphaStation 200 4/100, in the Biological Chemistry Department, John Innes Center. Crystal data are collected in Table 4.

Intensity data for **2** were processed with *C*₂ symmetry. However, it was later recognized that **1** and **2** are isostructural and that **2** was twinned by reflection in the plane *y* = 0, giving apparent *C*-centering of the cell. It was found to be necessary, in the refinement process, to constrain some of the bond dimensions about atoms on or close to the twinning plane, viz., Y, Mg, O(1), O(2), O(3), and C(57).

Acknowledgment. This work was supported by the European Commission: Marie Curie Fellowships, FP6-Mobility-5, Contract MEIF-CT-2003-500476. We are grateful to Dr. J. E. Davies of the Department of Chemistry, University of Cambridge, for the measurement and processing of the diffraction intensities for compound **2**.

Supporting Information Available: Full listing of crystallographic details for compounds **1**, **2**, **3**, and **5**. This material is available free of charge via the Internet at <http://pubs.acs.org>.

OM0505155

(12) Otwinowski, Z.; Minor, W. *Methods Enzymol.* **1997**, 276, 307.

(13) Blessing, R. H. *J. Appl. Crystallogr.* **1997**, 30, 421.

(14) Sheldrick, G. M. *Acta Crystallogr.* **1990**, A46, 467.

(15) Sheldrick, G. M. *SHELXL*, Program for Crystal Structure Refinement; University of Göttingen: Göttingen, Germany, 1997.

(16) *International Tables for X-ray Crystallography*; Kluwer Academic Publishers: Dordrecht, The Netherlands, 1992; Vol. C, pp 193, 219, 500.